

# Structural and magnetic properties of Fe clusters embedded in Ag matrix

HAO WANG

*Institute of Thin Film Science & Technology, Wuyi University, Jiangmen, Guangdong, 529020, People's Republic of China*

Evaporation–gas–aggregation (EGA) co-deposition for the preparation of thin films of Fe clusters embedded in a silver matrix is developed in this paper. Transmission electron microscope and electron diffraction investigations and X-ray energy spectrum show that Fe clusters are well encapsulated in silver coatings and are in the form of body centred cubic Fe and face centred cubic Ag in as-prepared samples. Vibrating sample magnetometer measurements reveal that samples show superparamagnetic behaviour and saturation magnetization increases with decreasing test temperature. At lower temperature, the coercivity is much higher than that of bulk  $\alpha$ -Fe, and it decreases with increasing test temperature. © 1998 Kluwer Academic Publishers

## 1. Introduction

In recent years, magnetic transition metal clusters of Fe, Co–Ni embedded in a kind of non-magnetic medium have gained increasing attention owing to properties that are quite different from those of bulk materials and thin films, such as size dependency, quantum confinement, superparamagnetic behaviour and giant magnetoresistance (GMR). These properties possess a variety of applications in the fields of high-density magnetic recording medium, catalysts, magnetoresistance sensors and computer read heads for high density magnetic recording and so on. The first example of nanoscale  $\alpha$ -Fe particles without surface contamination by magnetic iron oxide, but instead having Mg(Li) protective shells, has been achieved using a co-evaporation technique [1]. These well encapsulated samples show superparamagnetic and strong size dependency behaviour. After the discovery of GMR in a multilayer system [2] and in granular films [3,4]. GMR has also been discovered in ionized cluster-beam-deposited Fe–Ag embedded clusters [5] and epitaxially grown Fe–Ag and Co–Ag nanogranular films [6]. More recently, films of Co clusters, about 3 nm in diameter, embedded in a silver matrix have been produced via the low-energy cluster beam deposition technique (LECBD): a maximum GMR value of about 12% was obtained for a Co concentration close to the three-dimensional percolation threshold (about 20%) [7]. The first magnetic X-ray circular dichroism measurements (MXCD) on mesoscopic thin films of Co clusters embedded in a copper matrix, which are prepared by combining sputter–gas–aggregation (SGA) techniques with conventional magnetron sputtering, reveal that the magnetization of as-prepared samples depends on the average cluster size and concentration but, in all cases, is significantly less than

that of a thin cobalt film even at magnetic fields 4 T [8].

Based on the SGA technique for atomic cluster generation [9], a novel method, i.e. evaporation–gas–aggregation (EGA), for Fe–Ag embedded cluster preparation is developed in this paper. The morphology and microstructure of the as-prepared samples are investigated by transmission electron microscopy (TEM); magnetic properties were measured using a vibrating sample magnetometer (VSM).

## 2. Experimental procedure

The experimental arrangement is shown in Fig. 1, and consists of three main parts: a cluster generation region, a condensation region and a deposition chamber.

Under the collision of background gas (Ar), Fe atoms evaporate from source A, and small Fe clusters are formed in the cluster generation region. With flowing gas, small clusters and single Fe atoms move into the condensation region through an aperture. Then, quantitative large clusters are formed and these move directly into the deposition chamber, but most single atoms are pumped out via the oil pump. Thus, Fe clusters and Ag atoms evaporated from source B are deposited onto the substrate surface simultaneously, forming a thin film of Fe–Ag embedded clusters. In order to distinguish from other techniques, such as co-evaporation and co-sputtering, this method is named EGA co-deposition.

Samples are prepared on formvar foil for TEM study and on single crystal silicon (1 1 1) wafers for VSM measurement under the same deposition conditions, and at an Fe cluster beam deposition rate of about  $0.1 \text{ nm s}^{-1}$ .

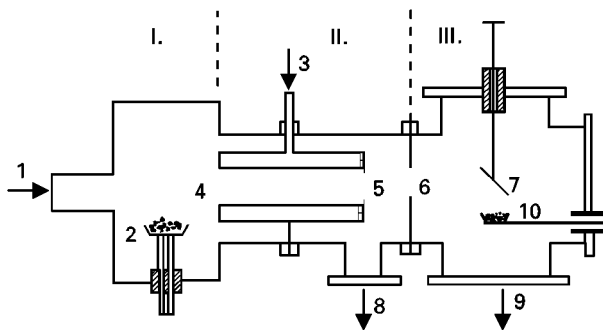


Figure 1 Experimental arrangement: I, cluster generation region; II, condensation region; III, deposition chamber. (1) Gas inlet, (2) evaporation source A, (3) liquid nitrogen inlet, (4–6) apertures, (7) substrate, (8) oil pump, (9) molecular pump, (10) evaporation source B.

### 3. Results and discussion

The morphology and electron diffraction pattern of the as-prepared Fe–Ag sample are shown in Fig. 2.

The morphology shows that Fe clusters are well dispersed in the silver matrix and are not strongly aggregated in the as-prepared sample. The size distribution of the Fe clusters is well fitted to a Gaussian distribution, centred around a mean size of 8.0 nm, with the normal difference,  $\sigma$ , being 0.5 nm (by statistical analysis from the data in the morphology photograph). The electron diffraction pattern shows that face centred cubic (fcc) Ag coatings are in polycrystalline form with (1 1 1), (2 2 0), (2 2 2) crystal planes and body centred cubic (bcc) Fe clusters with (1 1 0), (2 0 0), (1 1 2) crystal planes; but the Fe (2 0 0) and (1 1 2) crystal planes are coincident with the Ag (2 2 0), (2 2 2) crystal planes. No diffraction rings from other materials, such as iron oxides, have been observed. X-ray energy spectrum testing indicates that it mainly contains Fe and Ag elements, and the compositional ratio of Fe:Ag is 35:65. All these results reveal that phase separation between Fe and Ag has been partially achieved: Ag atoms tend to be on the surface of Fe clusters and form a protective coating around Fe clusters in the as-produced specimens. More detailed analysis shows that the lattice constants of different crystal planes in the Fe clusters have been shrinking at different degrees, the shrinking amounts compared with those of bulk Fe are 5.7, 1.3 and 0.8% for the (1 1 2), (2 0 0) and (1 1 0) crystal planes, respectively. The shrinking is due to the large ratio of surface atoms and to the cluster volume (additional pressure will be applied to Fe clusters for surplus surface atoms).

Fig. 3 shows the magnetization curves versus applied field  $H$ , at different temperatures. At 300 K, magnetization tends to be saturated at low field (about 0.06 T), and magnetic saturation is much lower than that of the bulk  $\alpha$ -Fe ( $220 \text{ e.m.u. g}^{-1}$  at 300 K). With decreasing temperature, saturation magnetization increases and reaches  $55 \text{ e.m.u. g}^{-1}$  at 150 K, and  $110 \text{ e.m.u. g}^{-1}$  at 85 K. Further magnetic studies for the sample show superparamagnetic behaviour, as identified by the magnetization versus  $H/T$  relationship. We consider these may be caused by the size effect of the Fe cluster. There is a critical size below which the

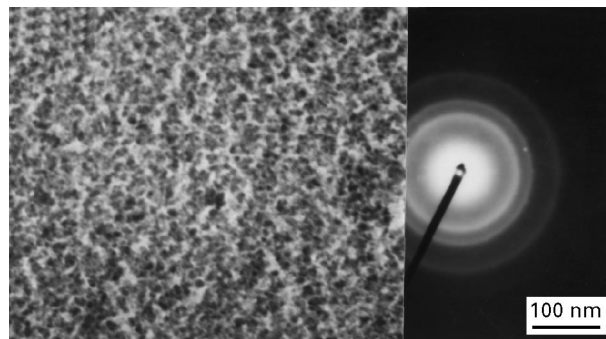


Figure 2 TEM–ED photograph of Fe–Ag embedded cluster: (a) TEM bright-field morphology (left) and (b) electron diffraction (ED) pattern (right).

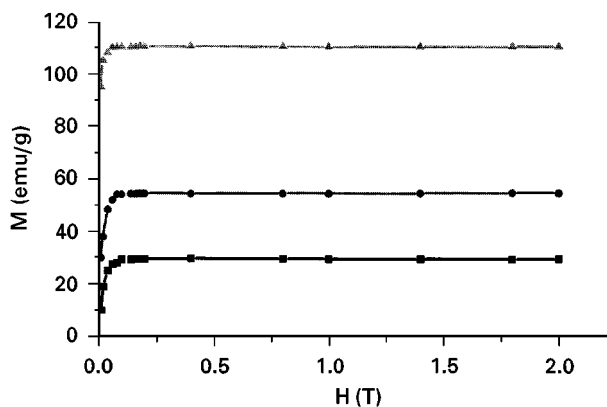


Figure 3 Magnetization versus applied field curve of Fe–Ag embedded clusters. —■—  $T = 300 \text{ K}$ , —●—  $T = 150 \text{ K}$ , —▲—  $T = 85 \text{ K}$ .

cluster can be in the state of a single magnetic domain. At a satisfactory temperature when the magnetic anisotropy energy barriers are overcome by thermal energy, the cluster would possess superparamagnetic relaxation. Here, the observed Fe cluster size (8 nm) is a little larger than the theoretical critical value of the  $\alpha$ -Fe particle (3.2 nm), which may be caused by the electronic structural difference between the Fe cluster at the quantum confined condition and ultrafine  $\alpha$ -Fe particle. The concentration of Fe clusters and boundary interaction between Fe clusters and silver coatings may also play an important role. For more accurate study, cluster size and its distribution should be measured and monitored *in situ* with a time-of-flight (TOF) mass spectrometer.

Coercivity measurements as a function of temperature are shown in Fig. 4, where we can see values decreasing from  $32.2 \times 10^3$  to  $8.8 \times 10^3 \text{ A m}^{-1}$  when the temperature increases from 100 to 300 K, and all of the values are larger than that of bulk Fe,  $6.4 \times 10^3 \text{ A m}^{-1}$ . The single domain cluster is self-magnetized at certain directions, which lead the uneasiness of magnetization of the whole sample, i.e. increasing coercivity. With increasing temperature, magnetic interaction between each single domain cluster is strengthened, thus coercivities of the whole sample decrease.

### 4. Conclusions

A novel method for Fe–Ag embedded cluster preparation is developed. Based on a TEM, electron

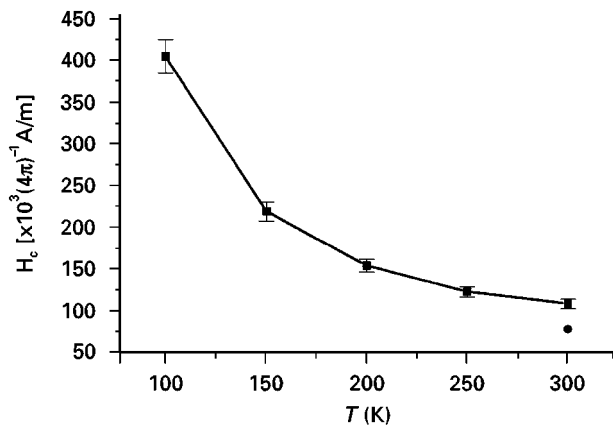


Figure 4 Coercivity versus temperature curve of Fe–Ag embedded clusters. —■— Fe/Ag, —●— bulk Fe.

diffraction and X-ray energy spectrum investigation, we can conclude that Fe clusters are well encapsulated in silver coatings and in polycrystalline form with bcc structure Fe and fcc structure Ag in as-deposited samples, in which surface oxidation and self-aggregation could be avoided effectively. VSM measurements reveal that the magnetic properties are dependent on the measurement temperature and are quite different from that of bulk  $\alpha$ -Fe.

## Acknowledgements

The financial support of National Post-doctoral Science Foundation and Natural Science Foundation of China are acknowledged with gratitude.

## References

1. K. J. KLABUMDE, D. ZHANG, G. N. GLAVEE, *et al.*, *Chem. Mater.* **6** (1994) 784.
2. M. N. BAIBICH, J. M. BROTO, A. FERT, *et al.*, *Phys. Rev. Lett.* **61** (1988) 2472.
3. A. BERKOWITZ, J. R. MITCHELL, M. J. COSSY, *et al.*, *ibid.* **68** (1992) 3745.
4. J. Q. XIAO, J. S. JIANG and C. L. CHIEN, *ibid.* **68** (1992) 3749.
5. K. SUMIYAMA, K. SUZUKI, S. A. MAKHLOUF, *et al.*, *Mater. Sci. Eng.* **B31** (1995) 133.
6. N. THANGARAJ, C. ECHER, K. M. KRISHNAN, *et al.*, *J. Appl. Phys.* **75** (1994) 6900.
7. A. PEREZ, P. MELINON, V. DUPUIS, *et al.*, *J. Phys. D, Appl. Phys.* **30** (1997) 709.
8. D. A. EASTHAM, Y. QIANG, T. H. MADDOCK, *et al.*, *J. Phys. Condens. Mater.* **9** (1997) L497.
9. H. HABERLAND, Z. INSEPOV, M. KARRAIS, *et al.*, *Mater. Sci. Eng.* **B19** (1993) 31.

Received 27 February 1997  
and accepted 23 June 1998